

Manuscript version: Author's Accepted Manuscript

The version presented in WRAP is the author's accepted manuscript and may differ from the published version or Version of Record.

Persistent WRAP URL:

<http://wrap.warwick.ac.uk/139983>

How to cite:

Please refer to published version for the most recent bibliographic citation information. If a published version is known of, the repository item page linked to above, will contain details on accessing it.

Copyright and reuse:

The Warwick Research Archive Portal (WRAP) makes this work by researchers of the University of Warwick available open access under the following conditions.

© 2020 Elsevier. Licensed under the Creative Commons Attribution-NonCommercial-NoDerivatives 4.0 International <http://creativecommons.org/licenses/by-nc-nd/4.0/>.



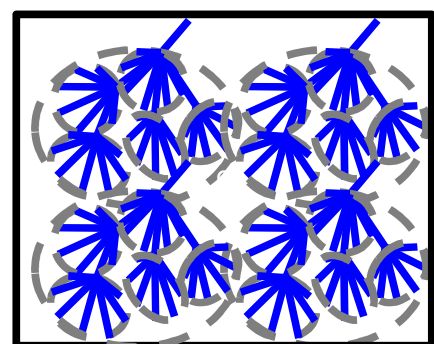
Publisher's statement:

Please refer to the repository item page, publisher's statement section, for further information.

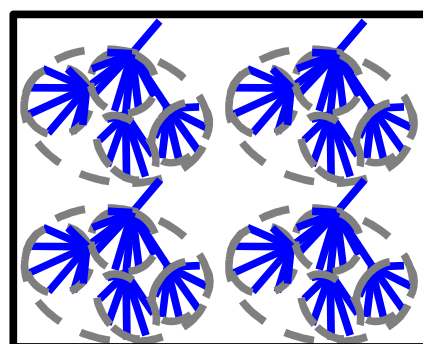
For more information, please contact the WRAP Team at: wrap@warwick.ac.uk.

CRedit author statement:

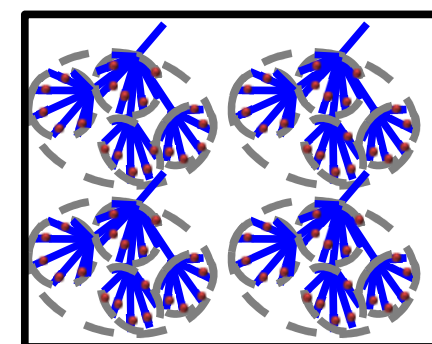
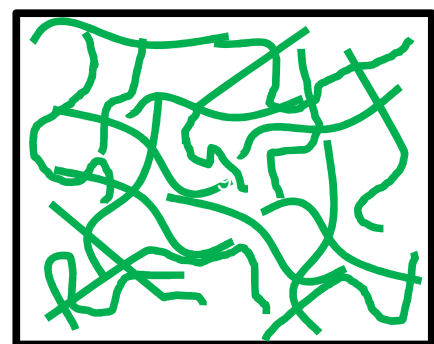
Pei Chen: Conceptualization, Methodology, Validation, Formal Analysis, Investigation, Resources, Data Curation, Writing - Original Draft, Visualization, Supervision, Project administration, Funding acquisition. **Yiling Zhang:** Methodology, Validation, Formal Analysis, Investigation. **Qian Qiao:** Methodology, Validation, Formal Analysis, Investigation. **Xiaoqi Tao:** Methodology, Validation, Formal Analysis, Investigation. **Peng Liu:** Conceptualization, Methodology, Validation, Formal Analysis, Investigation, Resources, Writing - Original Draft, Writing - Review & Editing, Visualization. **Fengwei Xie:** Conceptualization, Methodology, Validation, Formal analysis, Resources, Data Curation, Writing - Original Draft, Writing - Review & Editing, Visualization, Supervision, Project administration, Funding acquisition.

**Amylopectin**

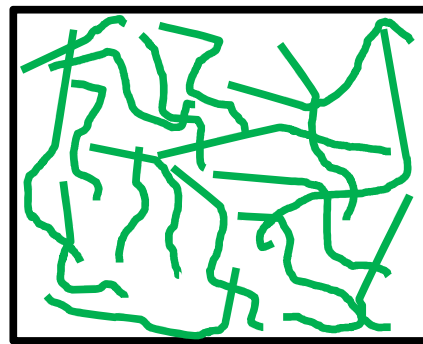
*Significant
decrease in
chain interaction*

**Acid-hydrolysed**

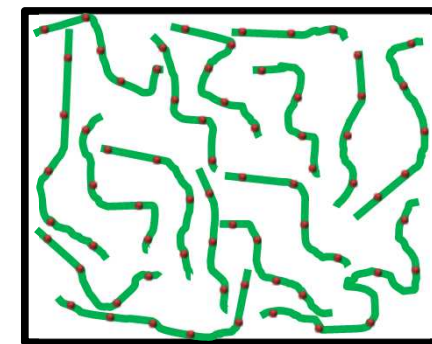
*Insignificant
decrease in
chain interaction*

**Hydroxypropylated****Amylose**

*Significant
decrease in
chain interaction*

**Acid-hydrolysed**

*Significant
decrease in
chain interaction*

**Hydroxypropylated**

1 **Comparison of the structure and properties of hydroxypropylated**
2 **acid-hydrolysed maize starches with different amylose/amylopectin contents**

3
4 Pei Chen ^a, Yiling Zhang ^a, Qian Qiao ^a, Xiaoqi Tao ^a, Peng Liu ^{b,c,*}, Fengwei Xie ^{d,e,**}

5
6 ^a *College of Food Science, South China Agricultural University, Guangzhou, Guangdong 510642, China*

7 ^b *School of Chemistry and Chemical Engineering, Guangzhou University, Guangzhou, Guangdong 510006,*
8 *China*

9 ^c *Fine Chemical Research Institute, Guangzhou University, Guangzhou, Guangdong 510006, China*

10 ^d *International Institute for Nanocomposites Manufacturing (IINM), WMG, University of Warwick, Coventry*
11 *CV4 7AL, United Kingdom*

12 ^e *School of Chemical Engineering, The University of Queensland, Brisbane, Qld 4072, Australia*

13
14 * Corresponding Author. Email: liu_peng@gzhu.edu.cn (P. Liu)

15 ** Corresponding Author. Email: d.xie.2@warwick.ac.uk; f.xie@uq.edu.au (F. Xie)

16
17

18 **Abstract**

19 Dually modified regular maize starch (RMS) and high-amylose maize starch (HAMS) were
20 successfully prepared by first acid hydrolysis and subsequently hydroxypropylation. The effects of
21 hydrolysis time (0–24 h) and propylene oxide (PO) content (10–30%) on the structure and
22 physicochemical properties were investigated. The molar substitution (MS) of HAMS samples (up to
23 0.163) was generally higher than that of RMS samples (up to 0.149), suggesting the higher reactivity
24 of amylose for hydroxypropylation. Besides, PO content had a greater influence on MS whereas the
25 effect of acid hydrolysis time was minor. For both starches, the dual modifications did not cause
26 apparent changes to the granule morphology but reduced gelatinisation temperatures and enthalpy;
27 and a higher PO content led to higher relative crystallinity. These results suggest that
28 hydroxypropylation occurred mainly on the surface of HAMS granules and had little influence on the
29 compact granular structure, whereas this reaction impacted the internal structure of RMS much more.
30 The rheological study shows the introduced hydroxypropyl bulky groups weakened the
31 entanglements between amylose chains or amylopectin chains with long branches. Thus, this work
32 provides insights into the rational design of modified starch products containing different
33 amylose/amylopectin contents with tailored properties.

34 *Keywords:* maize starch; hydroxypropylation; acid hydrolysis; rheological properties; intrinsic
35 viscosity; gelatinization

36 **1 Introduction**

37 Starch is a type of natural biomacromolecule formed by the photosynthesis of plants. It is an
38 abundant, cheap, biodegradable, and environmentally friendly resource and has great potential in a
39 diversity of applications such as food ingredients, pharmaceutical materials, and biodegradable
40 plastics (Yang et al., 2016). However, native starch has some drawbacks such as its insolubility in
41 water and easy retrogradation. Therefore, starch usually needs to be modified for specific and
42 enhanced applications (Liu, Ramsden, & Corke, 1999; Kaur, Singh, & Singh, 2004; Chun & Yoo,
43 2007; Lawal, 2011; Lee & Yoo, 2011).

44 Hydroxypropyl starch (HPS) is a popular modified starch product that has been widely used in
45 industry since the first patent about it published in 1968 (Toshio, 1968). Hydroxypropylation
46 introduces hydrophilic bulky groups to the starch backbone, which increases its solubility, paste
47 clarity, cohesiveness, freeze-thaw stability, and enzymatic digestibility (Lawal, 2011; Lee & Yoo,
48 2011). Due to the enhanced properties, HPS has found important applications in food (Miyazaki,
49 Van Hung, Maeda, & Morita, 2006), biodegradable films (Woggum, Sirivongpaisal, & Wittaya,
50 2015b), and pharmaceutical capsules (Zhang et al., 2013).

51 However, for HPS, it is challenging to achieve high molar substitution (MS) and the reaction is
52 usually limited on the granule surface (Fouladi & Mohammadi Nafchi, 2014). To improve the
53 reactivity, Fouladi & Mohammadi (Fouladi & Mohammadi Nafchi, 2014) have attempted a dual
54 modification method with a combination of acid hydrolysis and hydroxypropylation, which showed
55 synergistic effects on the functional properties (e.g. solubility) of sago starch. Li et al. (Li et al., 2018)
56 reported the superior gelling and gel properties of acid-hydrolysed and hydroxypropylated potato
57 starch.

58 The overall reactivity can be determined by not only the granule architecture (whether there are
59 channels in the granule) but also the reactivity of starch chains within the granule (Bemiller, 1997;
60 Kaur, Ariffin, Bhat, & Karim, 2012). Traditionally, depending on the chain structure, there are two
61 types of starch biomacromolecule identified, namely amylose and amylopectin (Chen, Yu, Chen, &
62 Li, 2006; Chen et al., 2009). Amylose is in the form of mainly long, linear chains with limited
63 branches, which tend to entangle with each other, while amylopectin has large amounts of
64 highly-branched, short chains with limited capability for entanglement (Liu, Yu, Xie, & Chen, 2006;
65 Liu et al., 2011). The molecular weight of amylose (10^5 – 10^6) is much lower than that of amylopectin
66 (10^7 – 10^9) (Pérez, Baldwin, & Gallant, 2009).

67 The research of starch in the last two decades has further revealed the difference between
68 high-amylose starch (HAS) and regular starch. Firstly, HAS contains not only amylose and
69 amylopectin, but also intermediate components, which is branched amylose chains or amylopectin
70 chains with long branches, functioning similarly as amylose (Jane et al., 1999; Vilaplana, Hasjim, &
71 Gilbert, 2012; Li, Gidley, & Dhital, 2019). Moreover, HAS presents a compact granule structure
72 with the absence of channels, which expresses the exo-corrosion pattern during the acid hydrolysis,
73 in contrast to the endo-corrosion pattern for waxy starch (Chen et al., 2006; Liu et al., 2006; Chen et
74 al., 2009; Xie et al., 2009; Wang et al., 2010; Li et al., 2011; Liu et al., 2011; Zou et al., 2012; Zhang
75 et al., 2014; Xie et al., 2015; Qiao et al., 2016; Chen, Xie, Zhao, Qiao, & Liu, 2017a; Liu et al.,
76 2017).

77 Therefore, it is interesting to compare the chemical reactivity between HAS and regular starch
78 for dual chemical modifications (acid hydrolysis and hydroxypropylation) and to investigate the
79 influence of such modification on the structure (morphology and crystalline structure) and

80 physicochemical properties (thermal and rheological properties) of these two starches, which has
81 formed the intention of this study. We particularly compared the effects of the starch chain structure
82 (highly-branched or linear) and the introduced hydroxypropyl groups on the rheological properties of
83 the modified starch solutions, which is scientifically and practically interesting.

84 **2 Materials and methods**

85 **2.1 Materials**

86 A regular maize starch (RMS) and a high-amylose maize starch (Gelose 80, about 80% amylose
87 content, as determined by the manufacturer) (HAMS) were purchased from National Starch Pty Ltd.
88 (Lane Cove, NSW, Australia). All chemicals used for the starch modification were of analytical
89 grade. Double-distilled water was used in all the experiments.

90 **2.2 Dual modifications of starch**

91 For acid hydrolysis, a starch slurry of 40% (w/v) concentration was prepared by adding 40 g of
92 starch (dry weight) into 100 g of 0.14 mol/L HCl solution. The slurry was incubated for different
93 times (6 h, 12 h, 18 h, and 24 h) in an oscillating incubator at 40 °C oscillated at 200 rpm. After that,
94 the pH of the starch slurries was adjusted to 5.5 with 5% (w/v) NaOH solution with continuous
95 stirring. The slurries were centrifuged (TDL-5-A, Shanghai Anting Scientific Instrument Factory,
96 China) at 5000 rpm for 10 min to remove the supernatant. The sediments were washed with distilled
97 water and then centrifuged at 5000 rpm for 10 min; and this procedure was performed three times.
98 The obtained starch was oven-dried overnight at 40 °C.

99 For hydroxypropylation, the hydrolysed starch slurries (20%, w/v) in flasks were added with 10%
100 anhydrous sodium sulphate with constant stirring. The resultant slurries were kept to be stirred and

101 heated at 40 °C in a water bath for 10 min. After the pH of the slurries was adjusted to 10.5 with 5%
102 (w/v) NaOH solution, certain amounts (10%, 20%, and 30%, based on the weight of starch dry basis)
103 of propylene oxide (PO) were added. The flasks were capped and the slurries were stirred at 40 °C for
104 24 h. Afterwards, the pH of the slurries was adjusted to 5.5 with 10% (w/v) HCl solution. The
105 slurries were centrifuged at 5000 rpm for 10 min to remove the supernatant. The sediments were
106 washed with distilled water and then centrifuged at 5000 rpm for 10 min; and this procedure was
107 performed three times. The starch was dried overnight in an oven at 40 °C.

108 All the dually modified starches were coded in the form of, for example, RMS-A6-P20 or
109 HAMS-A12-P10, where “RMS” or “HAMS” indicates the type of starch, A6 reflects the acid
110 hydrolysis time (6 h), and P20 means the added amount of PO (20%).

111 2.3 Characterisation

112 2.3.1 Intrinsic viscosity

113 For the determination of intrinsic viscosity ($[\eta]$), RMS and HAMS samples were dispersed in
114 1.0M KOH solutions. The solutions were stirred in a boiling water bath for 10 min, and then cooled
115 to room temperature (RT) and left overnight. Then, the solutions were centrifuged under 3000 r/min
116 for 6 min, and the final concentrations of the solutions were 2.6–6.0 mg/mL. $[\eta]$ was measured by an
117 Ubbelohde dilution capillary viscometer (size 37, Shanghai Shenyi Glass Instrument Factory, China),
118 which was immersed in a water bath maintained at 30.0±0.1 °C. The efflux time of solvent and
119 solutions were measured in triplicate and averaged. Then, $[\eta]$ can be calculated using the following
120 equation:

$$121 \quad [\eta] = \lim_{c \rightarrow 0} \frac{t - t_0}{c \times t_0} \quad (1)$$

122 where t is the efflux time of the starch solution (s), t_0 is the efflux time of the KOH solution (s), and c
123 represents the concentration of the starch solution (g/mL).

124 **2.3.2 Molar substitution (MS)**

125 The molar substitution (MS) for hydroxypropylation was determined using the method proposed
126 by Jones & Riddick (Jones & Riddick, 1957). This method involves the hydrolysis of the
127 hydroxypropyl group to propylene glycol, which is then dehydrated to propionaldehyde and acryl
128 alcohol. The products are reacted with ninhydrin to form a purple colour. The absorbance of this
129 purple solution was measured using a UV-visible spectrophotometer (UV-3802, Unico (Shanghai)
130 Instrument Co., Ltd., China) at $\lambda = 590$ nm with 1cm cuvettes to determine the concentration of
131 propylene glycol based on a standard curve that had been pre-established. The measured content (g)
132 of propylene glycol (W_{PG}) in 100 g of dually modified starch is converted into hydroxypropyl
133 equivalent using the following equation:

$$134 \quad MS = \frac{2.84W_{PG}}{100-W_{PG}} \quad (2)$$

135 **2.3.3 Scanning electron microscopy (SEM)**

136 The morphology of the starch granules was examined using a Philips XL30 FEG ESEM facility
137 (Koninklijke Philips N.V., Amsterdam, Netherlands). Before the examination, the samples were
138 coated with gold-palladium in a vacuum evaporator for 120 s. The samples were observed at a low
139 acceleration voltage of 15 kV.

140 **2.3.2 X-ray diffraction (XRD)**

141 X-ray diffraction (XRD) patterns of the starch samples were detected using a Rigaku Ultima IV
142 operating at 40 kV and 40 mA under Cu K α radiation. The data were collected from 4° to 40° 2θ at a
143 scanning speed of 2°/min. Relative crystallinity (X_c) was estimated using the MDI Jade 6.0 software

144 by deconvolution and fitting of crystalline peaks and the amorphous halo based on the XRD curves
145 between 4° and $40^\circ 2\theta$. Then, X_c was calculated by the following equation:

$$146 \quad X_c(\%) = \frac{A_c}{A_c + A_a} \times 100\% \quad (3)$$

147 where A_c and A_a are the integrated areas of all crystalline peaks and the amorphous halo,
148 respectively.

149 **2.3.3 Differential scanning calorimetry (DSC)**

150 The starch gelatinization behaviour was analysed using a PerkinElmer DSC 4000 facility
151 (PerkinElmer, Inc., Waltham, MA, USA). 3.5 mg (dry basis) of starch was weighed into a 40 μ L
152 aluminium pan and then distilled water was added to achieve a starch suspension containing 70% as
153 water. The samples were hermetically sealed and allowed to stand for 1 h at RT before DSC
154 measurements. Starch samples were heated at 5 $^\circ$ C/min from 20 to 130 $^\circ$ C under nitrogen.

155 **2.3.4 Rheological analyses**

156 Starch pastes (5%, w/v) were prepared by dispersing the starch samples (dry basis) in ZnCl₂
157 aqueous solutions (42 wt.% concentration in distilled water), which were heated at 50 $^\circ$ C in a water
158 bath for 20 min and then cooled down to RT. The capability of this ZnCl₂ aqueous solution to
159 completely dissolve starch (even HAMS) have been demonstrated before (Lin et al., 2016; Chen et
160 al., 2017b; Liu, Li, Shang, & Xie, 2019). The rheological properties of starch pastes were tested
161 using an MCR502 rheometer (Anton Paar GmbH, Austria) with a 60-mm-diameter cone-plate
162 geometry and a Peltier temperature control system. The distance between the plates was set at 1 mm.
163 The steady-state viscosity (η) was recorded in a shear-rate ($\dot{\gamma}$) range of 0–500 s^{-1} at a fixed
164 temperature of 25 $^\circ$ C. At least duplicate tests were performed for each sample. The rheological data
165 was fitted based on the power-law model in the following equation:

166 $\eta = K\dot{\gamma}^{n-1}$ (4)

167 where η is the flow viscosity (Pa s) of the starch solution, $\dot{\gamma}$ is the shear rate (s^{-1}), K is the
168 consistency (Pa s), and n is the power-law index.

169 2.3.7 Statistical Analysis

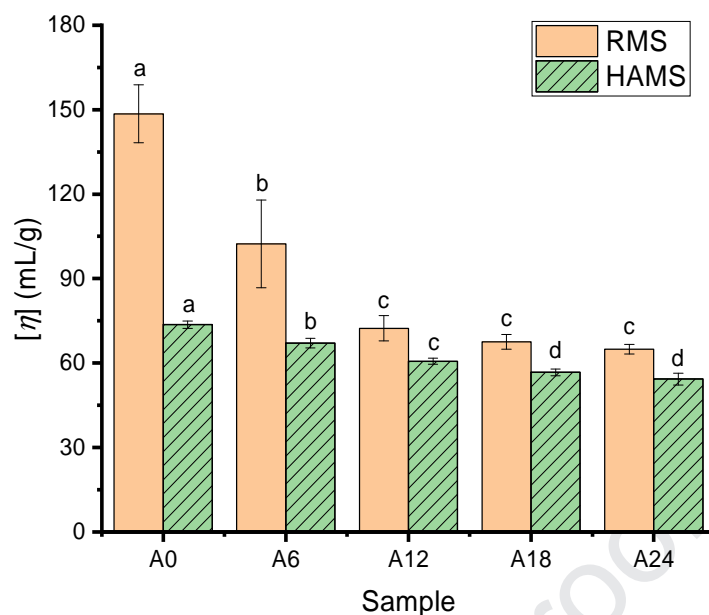
170 All the experiments were performed at least in triplicate and experimental data were analysed
171 using analysis of variance (ANOVA) and expressed as mean value \pm standard deviation. The
172 significant differences were determined using Duncan's HSD test ($p < 0.05$) with the SPSS 22.0
173 statistical software (SPSS Inc., Chicago, IL, USA).

174 3 Results and discussions

175 3.1 Intrinsic viscosity of acid hydrolysed RMS and HAMS

176 Intrinsic viscosity ($[\eta]$) is an important parameter reflecting the molecular size or mass of a
177 polymer in a given solvent at a certain temperature. Thus, it can be used to evaluate the influence of
178 hydrolysis time on starch (Trinh & Dang, 2019; Li et al., 2020). **Fig. 1** shows that both native RMS
179 and HAMS have higher $[\eta]$ than their modified counterparts and prolonged time of hydrolysis led to
180 reduced $[\eta]$. Besides, RMS samples had higher $[\eta]$ values than HAMS samples, which could be
181 attributed to the higher content of amylopectin in RMS. The molecular mass of amylopectin (10^8
182 Dalton) is much higher than that of amylose (10^6 Dalton) (Li et al., 2019).

183



184

185 **Fig. 1.** Intrinsic viscosity ($[\eta]$) of RMS and HAMS samples. The different letters indicate significant
 186 differences ($p \leq 0.05$).

187

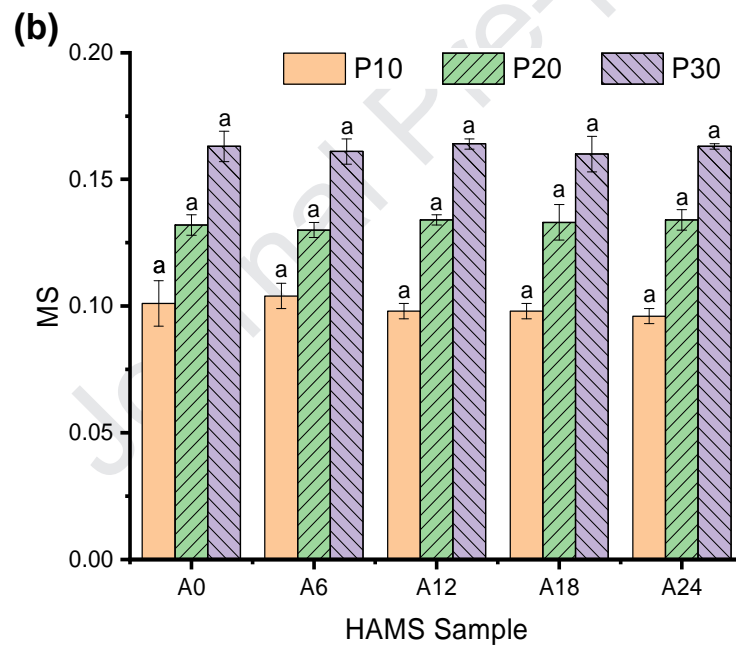
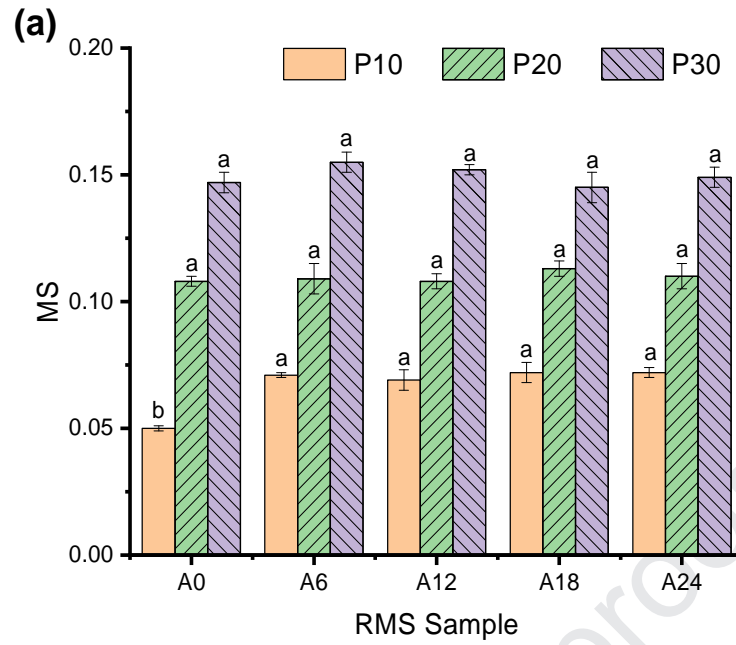
188 For RMS, $[\eta]$ changed rapidly during the early period of acid hydrolysis (especially the first 6 h)
 189 whereas the changes are small with further prolonged time. Similar kinetics has been reported
 190 previously (Kim, Lee, Kim, Lim, & Lim, 2012; Wang & Copeland, 2015), which can be explained
 191 by the first, fast hydrolysis of amorphous regions in starch granules while the crystallites are resistant
 192 to hydrolysis. Moreover, after 12 h of hydrolysis, there was no obvious change for $[\eta]$ ($p \leq 0.05$),
 193 indicating a stable state had been achieved during acid hydrolysis (Chen et al., 2017a). For HAMS,
 194 the acid hydrolysis resulted in more gradual and much smaller changes in $[\eta]$, indicating HAMS
 195 granules are more resistant to acid hydrolysis than RMS, which has been noted before (Nakazawa &
 196 Wang, 2003; Wang & Copeland, 2015). While the small pores in the periphery of the RMS granule
 197 could allow easy access of H^+ ions to the hilum, the HAMS granule has a compact periphery without
 198 pores, which could hinder the penetration of H^+ ions and thus, the acid hydrolysis (Chen et al., 2009;

199 Chen et al., 2011; Yang et al., 2016). Besides, Jayakody et al. (Jayakody & Hoover, 2002; Jane, 2006)
200 suggested that, in B-type starches, strong interaction exists between double helices, which are formed
201 in crystallites to a larger extent by intertwining with linear amylose chains, whereas for A-type
202 starches, the double helices in crystallites are constituted mainly by the intertwining of the outer
203 branches of amylopectin and their interaction is relatively weak. This may also explain the greater
204 resistance of HAMS, which is a B-type starch, against the acid hydrolysis. Besides, after 18 hours,
205 the hydrolysed HAS also reached a stable stage ($p \leq 0.05$).

206 **3.2 MS of modified RMS and HAMS**

207 **Fig. 2** shows the MS results of the native and modified starch samples. Among the P10 series of
208 RMS samples, RMS-A6-P10 had an apparently higher MS value than RMS-A0-P10. Similar
209 phenomena were observed in previous studies (Wang & Wang, 2001; Wang, Truong, & Wang, 2003;
210 Zhang et al., 2017; Jiang et al., 2018). In this regard, acid hydrolysis could make more active
211 hydroxyl groups in starch granules available for reaction with PO, leading to higher MS (Zhang et al.,
212 2017; Jiang et al., 2018). Nevertheless, further acid hydrolysis (from A6 to A24) did not cause
213 significant changes to MS ($p \leq 0.05$). This well corresponds to the $[\eta]$ trend. On the other hand,
214 when the PO content was high (for the P20 and P30 series), there was no significant variation in MS
215 among the samples with or without acid hydrolysis (from A0 to A24) ($p \leq 0.05$). Given this, it is
216 likely that when the PO content is high enough, PO can penetrate starch granules effectively for
217 reaction with active hydroxyl groups. A similar phenomenon was reported for sago starch (Fouladi &
218 Mohammadi Nafchi, 2014).

219



220

221

222

Fig. 2 Molar substitution (MS) of dually modified starches for RMS (a) and HAMS (b). The

223

different letters indicate significant differences ($p \leq 0.05$).

224

225 For HAMS samples, the MS was only affected by PO content but not apparently influenced by
226 acid hydrolysis time ($p \leq 0.05$). This can be explained by the low susceptibility of HAMS granules to
227 acid hydrolysis as shown by the $[\eta]$ data.

228 Also, it is interesting to observe that the MS values of HAMS were generally higher than those
229 of RMS irrespective of acid hydrolysis time. This may indicate the high reactivity of starch chains,
230 especially amylose or intermediate components, which has lower molecular mass, in the HAMS
231 granule. HAMS presents the exo-corrosion pattern during acid hydrolysis. As a result, under the
232 alkaline condition ($\text{pH} = 10.5$) for hydroxypropylation, OH^- ions could weaken the hydrogen
233 bonding between starch chains and assist PO penetration. Therefore, it is likely that PO penetration
234 did not rely on the channels or pores on the granule surface, and the MS is predominately influenced
235 by PO content. Similarly, for potato starch subjected to hydroxypropylation, amylose was found to
236 be modified to a greater extent than amylopectin (Kavitha & BeMiller, 1998).

237 **3.3 Morphology of modified RMS and HAMS**

238 The morphologies of native RMS and HAMS have been widely reported before. Native RMS
239 has spherical shapes with surface depressions and pores (Chen et al., 2006; Sujka & Jamroz, 2009;
240 Chen et al., 2017a) and native HAMS granules appear to be smooth with elliptical or rounded shapes
241 (Chen et al., 2006; Chen et al., 2017a). Compared with these native starches, **Fig. 3** shows that the
242 dual modifications did not apparently vary the granule morphology including the shape and size for
243 both RMS and HAMS. The starch granules were largely maintained under either the acid or alkaline
244 treatment.

245

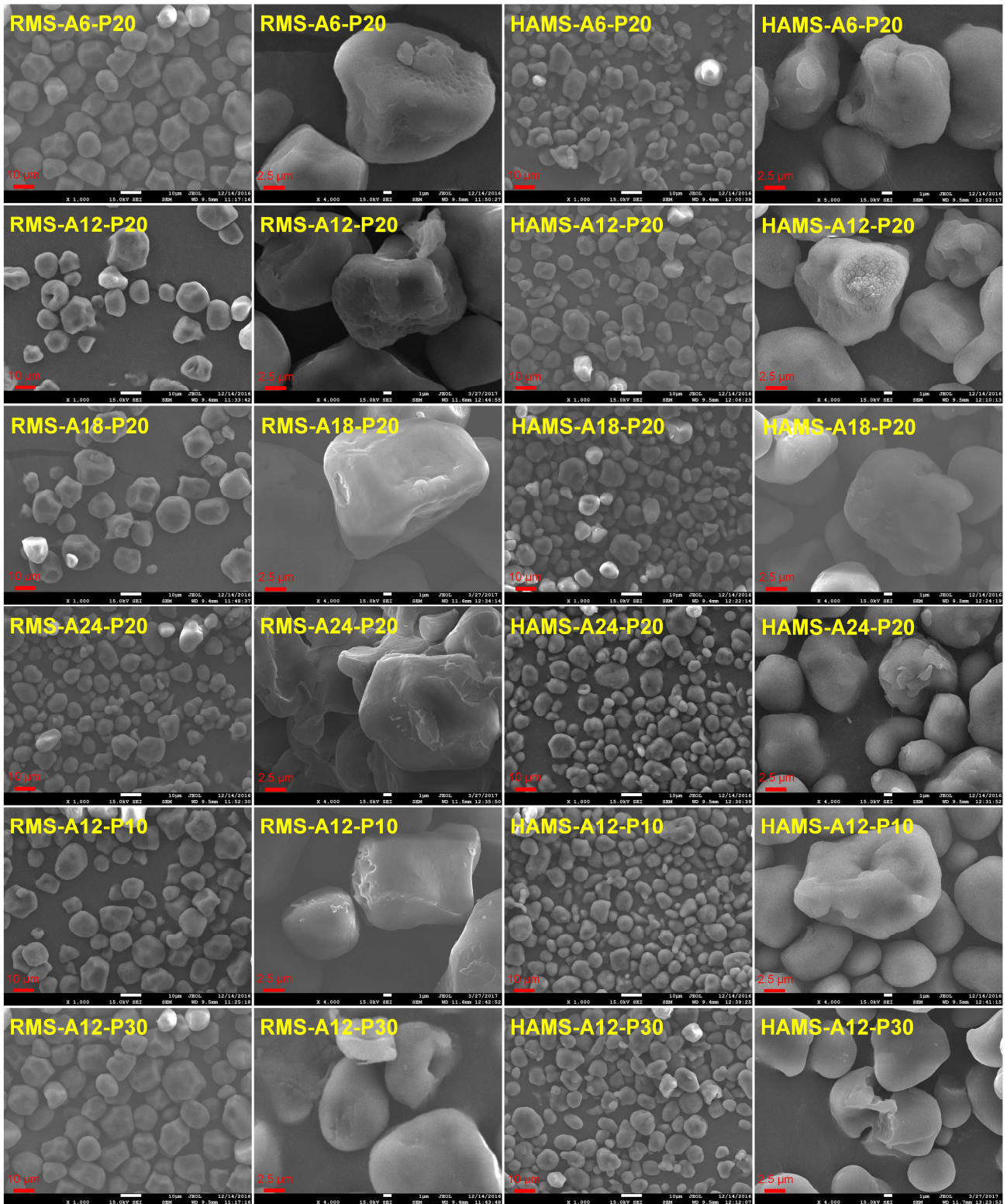


Fig. 3 SEM images of dually modified RMS and HAMS samples.

246

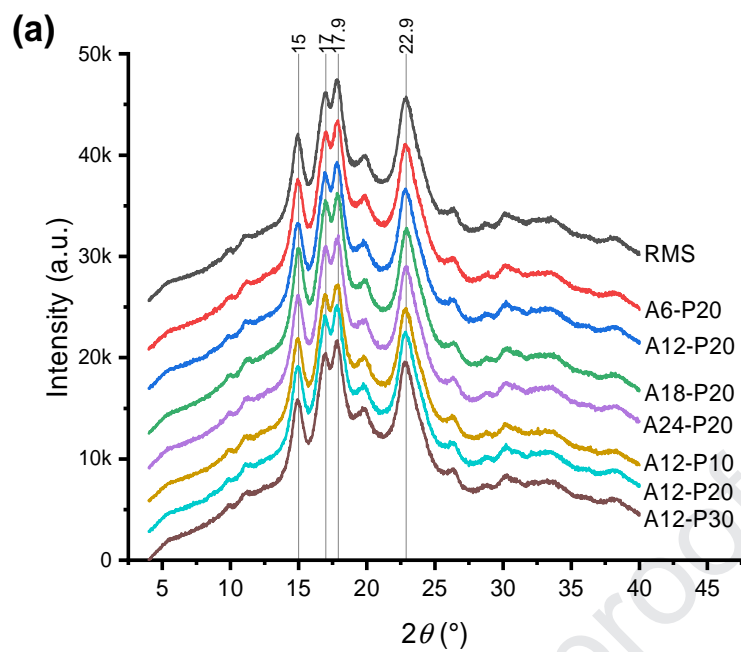
247

248

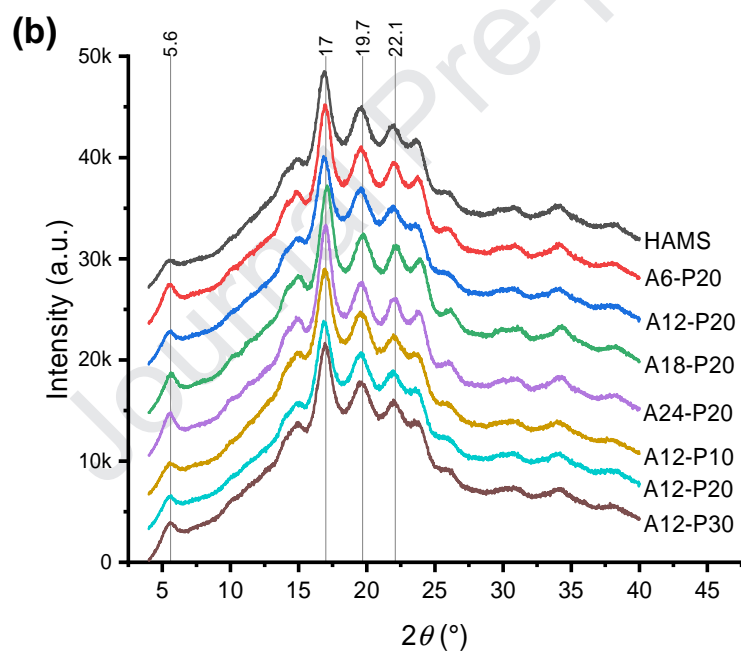
249 **Fig. 3** shows the acid hydrolysis with prolonged time did not cause apparent variation to the
250 granule morphology. In contrast, a higher content PO led to significant changes in the granule
251 morphology, such as the appearance of deep grooves on the granules of RMS-A12-P30 and the
252 fragmentation of granules for HAMS-A12-P30. These types of erosion should be attributed to the
253 chemical treatment (Hazarika & Sit, 2016). Similar results have been observed in the study by Kaur
254 et al. (Kaur et al., 2004), where potato starch granules treated with 10% PO showed the apparently
255 altered granule structure with folding, depressions, fragmentation, and/or deep grooves. They
256 proposed that hydroxypropylation mainly occurred in the less organised central region of the granule.
257 Since both HAMS and potato starch have B-type crystallinity with no pores on the surface,
258 hydroxypropylation is likely to have occurred in the depression regions of the granules.

259 **3.4 Crystalline structure of modified RMS and HAMS**

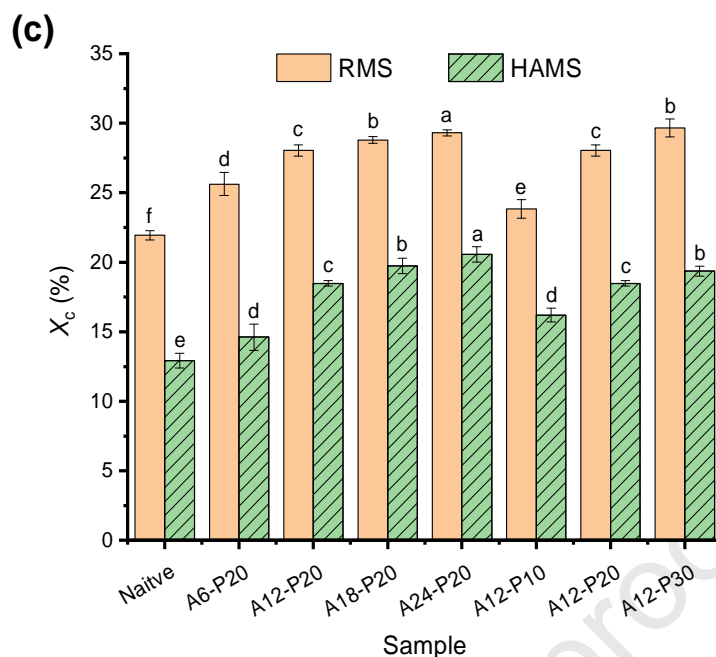
260 **Fig. 4(a)** and **(b)** show the XRD patterns for the native and modified starch samples. Native
261 RMS shows the A-type XRD pattern with strong reflections at 2θ of 15.0° , 17.0° , 17.9° , and 22.9° ,
262 and native HAMS exhibits the B-type XRD pattern, which is inferred from four main reflections at
263 2θ of 5.6° , 17.0° , 19.7° , and 22.1° (Cheetham & Tao, 1998; Tan, Flanagan, Halley, Whittaker, &
264 Gidley, 2007; Lopez-Rubio, Flanagan, Gilbert, & Gidley, 2008). For both RMS and HAMS, the dual
265 modifications did not cause any significant changes to the XRD patterns. Similarly, a previous study
266 (Jiang et al., 2018) showed no significant difference in the XRD pattern between native and
267 acid-thinned starches, meaning the mild acid treatment could not apparently alter starch crystallites.



268



269



270

271 **Fig. 4.** (a) and (b) XRD patterns for naive and modified RMS and HAMS, respectively; (c) Relative272 crystallinity (X_c) of native and modified RMS and HAMS. The different letters indicate significant273 differences ($p \leq 0.05$).

274

275 The X_c values of the native and modified starches are plotted in **Fig. 4(c)**. Native RMS had $X_c =$ 276 $21.9 \pm 0.3\%$ and HAMS had $X_c = 12.9 \pm 0.5\%$, similar to the data reported elsewhere (Chen et al.,

277 2017a; Liu et al., 2019; Li et al., 2020). The modified RMS and HAMS samples followed similar

278 trends of variation in X_c . For both starches, X_c increased with longer time of acid hydrolysis (from

279 A0-P20 to A24-P20) and a higher PO content for hydroxypropylation. This variation can be

280 explained that both hydrolysis and hydroxypropylation takes place in the amorphous regions (Wang

281 & Wang, 2001; Jayakody & Hoover, 2002; Wang et al., 2003; Zhang et al., 2017), and the reduction

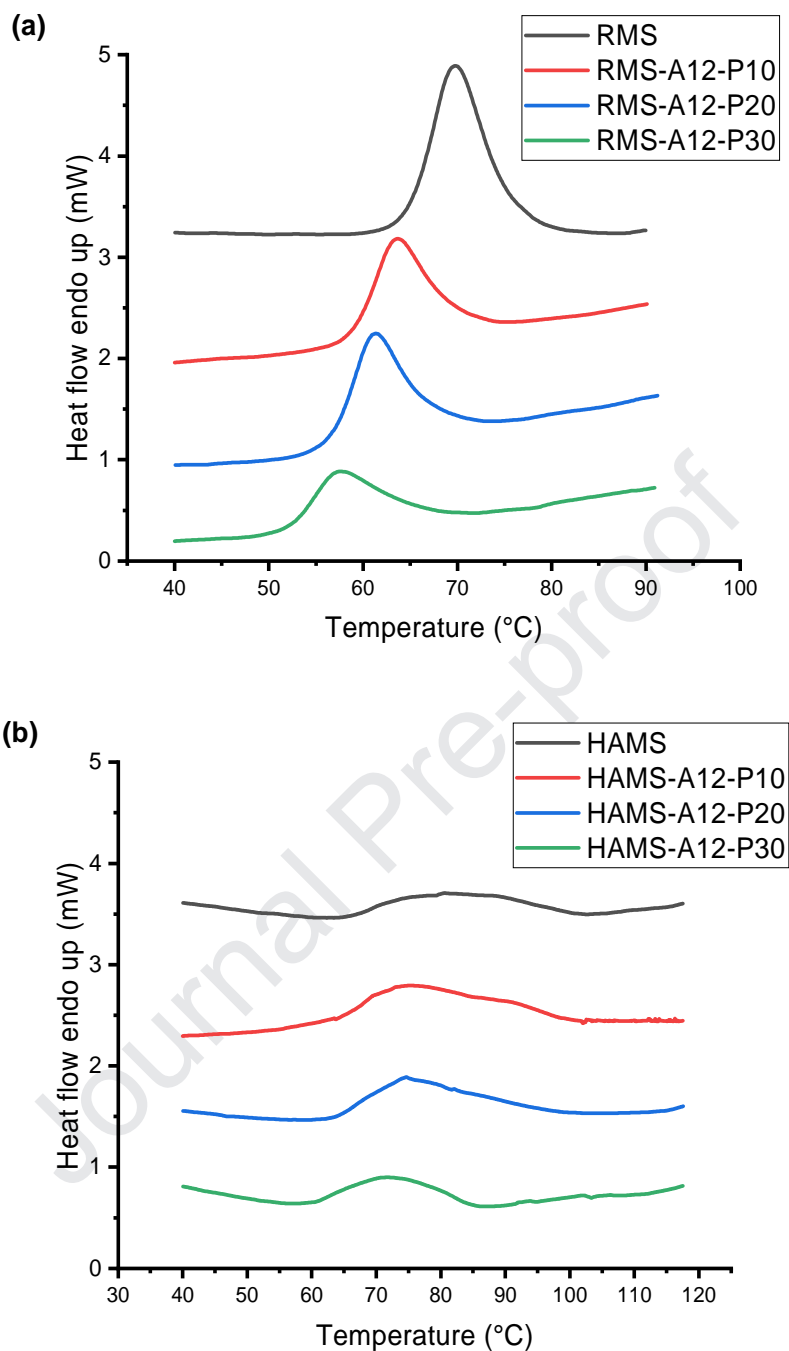
282 in amorphous content means higher X_c for the total samples.

283 3.5 Gelatinisation of modified RMS and HAMS

284 **Fig. 5** shows the DSC curves for the native and modified starch samples, with associated
285 gelatinisation parameters shown in **Table 1**. For both RMS and HAMS, increasing PO content led to
286 decreases in the gelatinisation onset and conclusion temperatures (T_o and T_c) as well as enthalpy
287 change (ΔH). In this regard, the introduction of hydroxypropyl groups could reduce the hydrogen
288 bonding between starch chains, destroy double helices, and make it easier for starch granules to
289 undergo swelling and melting of crystallites, leading to reduced gelatinisation temperatures and
290 enthalpy change (Seow & Thevamalar, 1993; Liu et al., 1999; Kaur et al., 2004; Chuenkamol,
291 Puttanlek, Rungsardthong, & Uttapap, 2007; Gunaratne & Corke, 2007; Lawal, 2009, 2011; Lee &
292 Yoo, 2011; Woggum, Sirivongpaisal, & Wittaya, 2015a). Moreover, for RMS, with a higher PO
293 content, the difference in T_o and T_c between samples are obvious, but for HAMS, the difference is
294 small between P10 and P20 samples and becomes obviously between P20 and P30 samples. This
295 result can be attributed to the different reaction site of hydroxypropylation between HAMS and
296 RMS.

297 Specifically, for HAMS, which presents the exo-corrosion pattern during acid hydrolysis,
298 hydroxypropylation should occur mainly on the surface of granules but have little influence on the
299 compact granular structure. As a result, the T_o and T_c values between P10 and P20 samples are
300 similar to each other. The compact granular structure could only be weakened with a large number of
301 hydroxypropyl groups introduced. On the other hand, for RMS, since it displays an endo-corrosion
302 pattern during acid hydrolysis, hydroxypropylation strongly influenced its inner structure of granules,
303 leading to apparent changes in T_o and T_c .

304



305

306

307

Fig. 5. DSC curves for native and modified RMS (a) and HAMS (b) samples.

308

Table 1. Onset temperature (T_o), conclusion temperature (T_c) and enthalpy change (ΔH) of

310

gelatinisation measured by DSC for native and modified RMS and HAMS samples.

Sample	T_o (°C)	T_c (°C)	ΔH (J/g)
--------	------------	------------	------------------

RMS	59.73±0.36 ^c	84.94±0.06 ^c	13.17±0.33 ^a
RMS-A12-P10	54.99±0.06 ^e	76.32±0.30 ^f	10.11±0.28 ^c
RMS-A12-P20	51.86±0.18 ^f	75.94±0.17 ^f	11.08±0.34 ^{bc}
RMS-A12-P30	49.02±0.13 ^g	72.60±0.12 ^g	8.44±0.09 ^d
HAMS	64.16±0.06 ^a	102.75±0.06 ^a	11.89±0.39 ^{ab}
HAMS-A12-P10	63.56±0.42 ^a	101.10±0.23 ^c	12.45±0.31 ^{ab}
HAMS-A12-P20	62.55±0.12 ^b	101.86±0.13 ^b	11.18±0.31 ^{bc}
HAMS-A12-P30	58.26±0.18 ^d	86.96±0.24 ^d	8.63±0.92 ^d

311 Different letters in the same column indicate statistical significance ($p < 0.05$).

312

313 Since the ΔH is the enthalpy for the phase transition of crystallinity, it is interesting to see that a
 314 high PO content caused an increase in X_c but a decrease in ΔH . Gelatinisation reflects the loss of
 315 molecular order (helical structures) rather than that of crystallinity (Cooke & Gidley, 1992). The
 316 introduction of hydroxypropyl groups could weaken the hydrogen bonding in helical structures and
 317 thus, reduce the enthalpy change. Similarly, hydroxypropylated acid-hydrolysed sago starch also
 318 shows apparently reduced gelatinisation temperature and enthalpy change (Fouladi & Mohammadi
 319 Nafchi, 2014).

320 3.6 Rheological properties of modified RMS and HAMS

321 Since the T_c values for the modified HAMS samples are still higher than 100 °C, it is difficult to
 322 obtain their homogeneous gelatinised solutions in water. Thus, a ZnCl₂ aqueous solution of 42 wt.%
 323 concentration was used to dissolve the starch samples fully (Lin et al., 2016; Chen et al., 2017b; Liu
 324 et al., 2019) for studying the rheological properties of the modified starch solutions.

325 **Fig. 5** shows the viscosity–shear rate curves for modified RMS and HAMS samples. All the
 326 samples displayed shear-thinning behaviour in the $\dot{\gamma}$ range in question (10–500 s⁻¹) and can be

327 considered as the pseudo-plastic fluids. Accordingly, the relationship between η and $\dot{\gamma}$ can be fitted
 328 using a power-law model (Eq. (4)) and the calculated parameters are listed in Table 2.

329

330

331

332

333

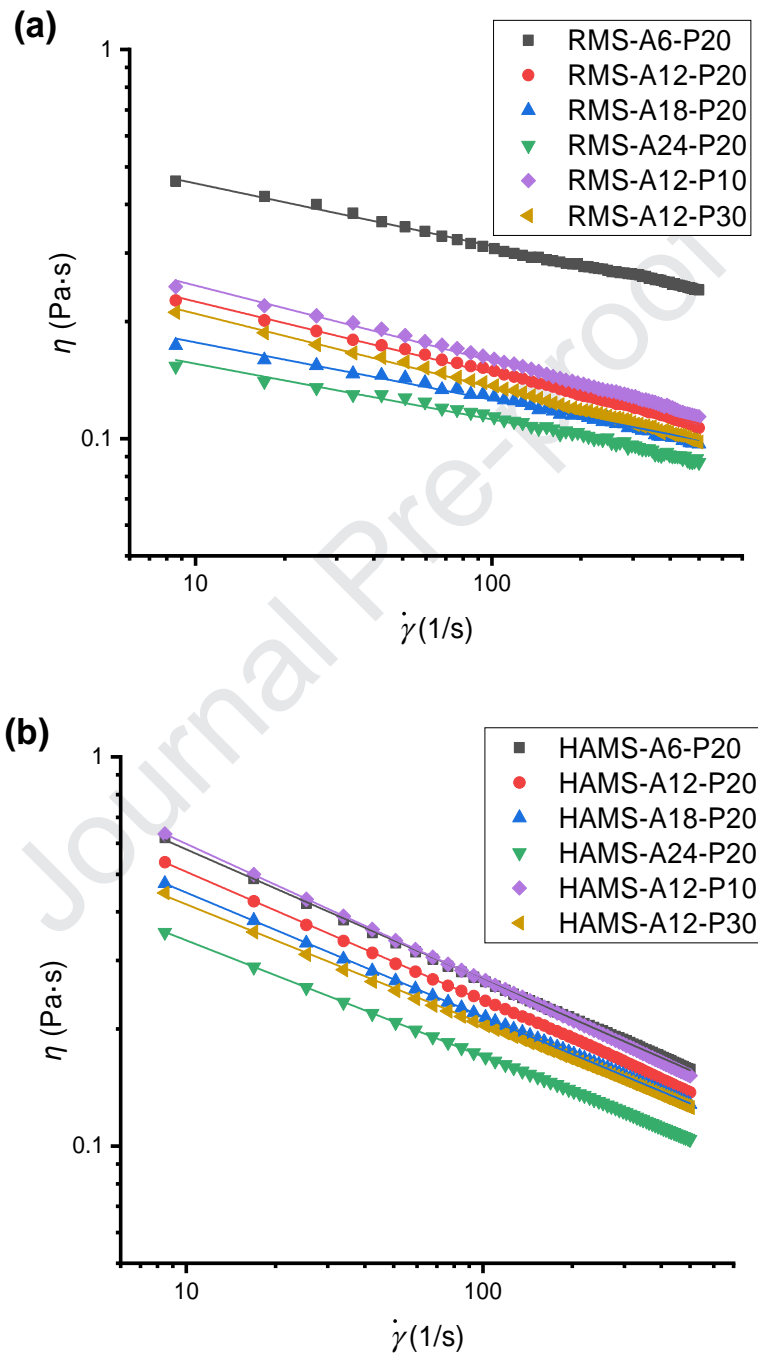


Fig. 6. Viscosity–shear rate curves for modified RMS and HAMS samples.

334

Table 2. Power-law parameters for modified RMS and HAMS samples.

Samples	K (Pa·s)	n
RMS-A6-P20	0.66±0.01 ^b	0.83±0.01 ^{def}
RMS-A12-P20	0.34±0.01 ^a	0.82±0.001 ^{bcdef}
RMS-A18-P20	0.23±0.02 ^a	0.85±0.01 ^{ef}
RMS-A24-P20	0.21±0.01 ^a	0.86±0.01 ^f
RMS-A12-P10	0.37±0.03 ^a	0.81±0.01 ^{bcdef}
RMS-A12-P30	0.31±0.08 ^a	0.82±0.03 ^{cdef}
HAMS-A6-P20	1.15±0.14 ^{de}	0.70±0.05 ^{ab}
HAMS-A12-P20	0.95±0.19 ^{cd}	0.71±0.06 ^{abc}
HAMS-A18-P20	0.81±0.17 ^{bc}	0.73±0.07 ^{abcd}
HAMS-A24-P20	0.60±0.09 ^b	0.75±0.07 ^{abcdef}
HAMS-A12-P10	1.25±0.13 ^e	0.69±0.06 ^a
HAMS-A12-P30	0.74±0.15 ^{bc}	0.74±0.05 ^{abcde}

335

Different letters in the same column indicate statistical significance ($p < 0.05$).

336

337

338

339

340

341

342

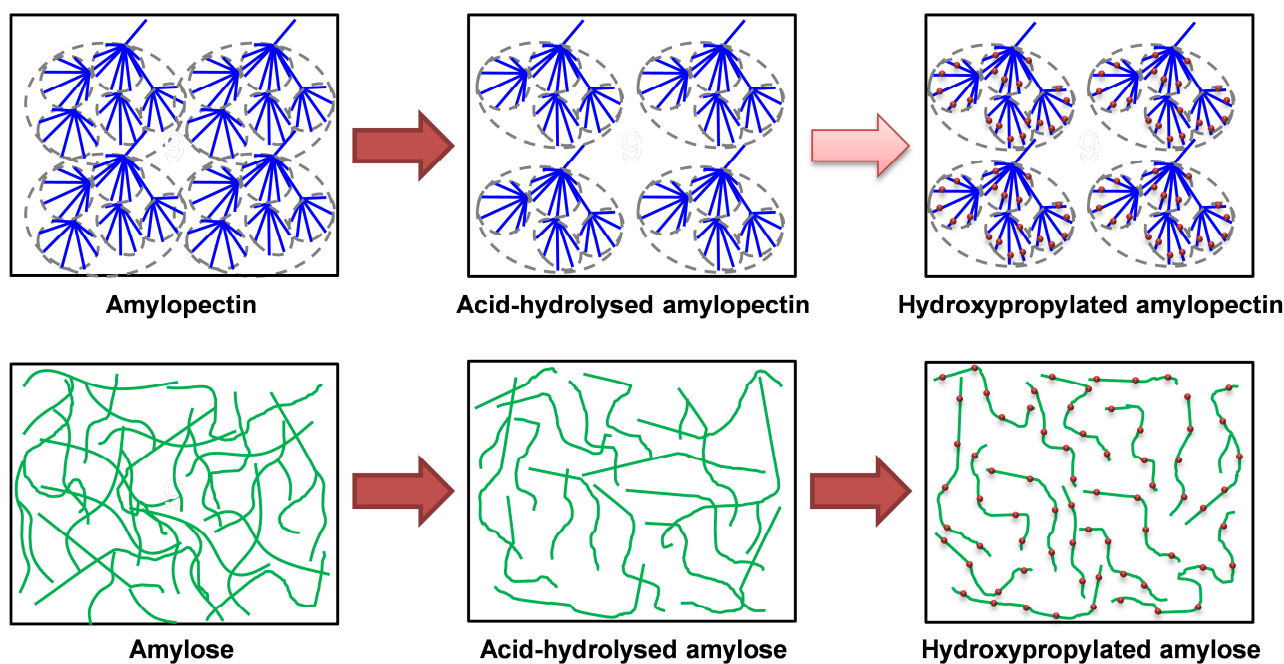
343

344

345

346

The modified HAMS samples had higher viscosities and lower n values than those of the modified RMS samples, indicating greater shear-thinning behaviour and stronger chain interaction for the former. The different rheological behaviours of the RMS and HAMS samples could be attributed to the different conformations of amylose (or amylopectin with long branches) and amylopectin in a solution. Specifically, the interaction between amylopectin chains can be limited by the steric hindrance provided by the large amounts of short and highly-branched side chains which are inflexible, whereas the interaction and entanglement between amylose (or amylopectin with long branches) chains can be easier (**Fig. 6**) (Yu & Christie, 2005; Tajuddin, Xie, Nicholson, Liu, & Halley, 2011).



347

348

349

350

351

352

353

354

355

356

357

358

359

360

361

Fig. 6. Schematic representation of chain conformations of amylose (or amylopectin with long branches) and amylopectin in a dissolved state. Arrows of dark red colour indicate a significant change in chain interaction whereas arrows of light red colour mean the change in chain interaction is insignificant.

It can be seen from **Table 2** that for both RMS and HAMS, acid hydrolysis and hydroxypropylation did not cause significant changes to n and thus, to the shear thinning behaviour. However, for both starches, K apparently decreased with longer time of acid hydrolysis, meaning a reduced extent of chain interaction. For HAMS, hydroxypropylation also significantly decreased K whereas this effect was not apparent for RMS. In this regard, we propose that the introduction of hydroxypropyl groups onto the amylose (or amylopectin with long branches) chains can effectively decrease the chain interaction and entanglement and thus, the solution viscosity. However, the introduction of hydroxypropyl groups onto the amylopectin chains have a limited effect to reduce the chain interaction and entanglement as these have already been largely constrained by the steric

362 hindrance provided by the inflexible short branches. These different effects of the dual modifications
363 on the chain interaction and entanglement of RMS and HAMS are schematically shown in **Fig. 6**.

364 **4 Conclusion**

365 In this work, we have revealed the different effect of a dual modification method (i.e. first acid
366 hydrolysis and subsequently hydroxypropylation) on the structure and properties of RMS and HAMS.
367 Firstly, for both starches, PO content had a greater influence on MS whereas the effect of acid
368 hydrolysis time was minor. In this regard, the alkaline treatment could swell starch granules and
369 facilitate the chemical reaction. Secondly, the MS values of HAMS were generally higher than those
370 of RMS irrespective of acid hydrolysis time. This indicates the high reactivity of amylose or
371 intermediate components, which has a lower molecular mass in HAMS. In addition, from the results
372 of gelatinisation temperatures (T_o and T_c) and enthalpy change (ΔH), it can be deduced that, for
373 HAMS, with the exo-corrosion pattern during acid hydrolysis, hydroxypropylation occurred mainly
374 on the granule surface but had little influence on the compact granular structure. Moreover, the
375 rheological results indicate that hydroxypropylation had very different effects on starch chains due to
376 their conformation in the solution. For amylose chains or amylopectin chains with long branches, the
377 introduced hydroxypropyl groups weakened the chain interaction and entanglement. Therefore, the
378 shear-thinning behaviour for these types of chains was much greater than amylopectin chains with
379 short branches.

380 The new understandings obtained from this work could provide insights into the rational design
381 of modified starch products containing different amylose/amylopectin contents with tailored
382 properties.

383 Acknowledgements

384 This research was funded by the China Postdoctoral Science Foundation (grant No.
385 2017M612679), the Sailing Scheme of Guangdong Province (grant No. 2017YT05H077), the
386 Guangxi Key Laboratory for Polysaccharide Materials and Modification, Guangxi University for
387 Nationalities (grant No. GXPSMM18ZD-02), and the Natural Science Foundation of Guangdong
388 Province (project No. 2018A0303130048). F. Xie acknowledges support from the European Union's
389 Horizon 2020 research and innovation programme under the Marie Skłodowska-Curie grant
390 agreement No. 798225.

391

392 References

- 393 Bemiller, J. N. (1997). Starch modification: Challenges and prospects. *Starch - Stärke*, 49, 127-131.
- 394 Cheetham, N. W. H., & Tao, L. (1998). Variation in crystalline type with amylose content in maize starch
395 granules: An x-ray powder diffraction study. *Carbohydrate Polymers*, 36, 277-284.
- 396 Chen, P., Xie, F., Zhao, L., Qiao, Q., & Liu, X. (2017a). Effect of acid hydrolysis on the multi-scale structure
397 change of starch with different amylose content. *Food Hydrocolloids*, 69, 359-368.
- 398 Chen, P., Yu, L., Chen, L., & Li, X. (2006). Morphology and microstructure of maize starches with different
399 amylose/amylopectin content. *Starch/Stärke*, 58, 611-615.
- 400 Chen, P., Yu, L., Simon, G., Petinakis, E., Dean, K., & Chen, L. (2009). Morphologies and microstructures of
401 cornstarches with different amylose-amylopectin ratios studied by confocal laser scanning microscope.
402 *Journal of Cereal Science*, 50, 241-247.
- 403 Chen, P., Yu, L., Simon, G. P., Liu, X., Dean, K., & Chen, L. (2011). Internal structures and phase-transitions
404 of starch granules during gelatinization. *Carbohydrate Polymers*, 83, 1975-1983.

- 405 Chen, X., Liu, P., Shang, X., Xie, F., Jiang, H., & Wang, J. (2017b). Investigation of rheological properties
406 and conformation of cassava starch in zinc chloride solution. *Starch - Stärke*, 69, 1600384.
- 407 Chuenkamol, B., Puttanlek, C., Rungsardthong, V., & Uttapap, D. (2007). Characterization of low-substituted
408 hydroxypropylated canna starch. *Food Hydrocolloids*, 21, 1123-1132.
- 409 Chun, S.-Y., & Yoo, B. (2007). Effect of molar substitution on rheological properties of hydroxypropylated
410 rice starch pastes. *Starch - Stärke*, 59, 334-341.
- 411 Cooke, D., & Gidley, M. J. (1992). Loss of crystalline and molecular order during starch gelatinisation: Origin
412 of the enthalpic transition. *Carbohydrate Research*, 227, 103-112.
- 413 Fouladi, E., & Mohammadi Nafchi, A. (2014). Effects of acid-hydrolysis and hydroxypropylation on
414 functional properties of sago starch. *International Journal of Biological Macromolecules*, 68,
415 251-257.
- 416 Gunaratne, A., & Corke, H. (2007). Functional properties of hydroxypropylated, cross-linked, and
417 hydroxypropylated cross-linked tuber and root starches. *Cereal Chemistry*, 84, 30-37.
- 418 Hazarika, B. J., & Sit, N. (2016). Effect of dual modification with hydroxypropylation and cross-linking on
419 physicochemical properties of taro starch. *Carbohydr Polym*, 140, 269-78.
- 420 Jane, J.-I. (2006). Current understanding on starch granule structures. *Journal of Applied Glycoscience*, 53,
421 205-213.
- 422 Jane, J., Chen, Y. Y., Lee, L. F., McPherson, A. E., Wong, K. S., Radosavljevic, M., & Kasemsuwan, T.
423 (1999). Effects of amylopectin branch chain length and amylose content on the gelatinization and
424 pasting properties of starch. *Cereal Chemistry*, 76, 629-637.
- 425 Jayakody, L., & Hoover, R. (2002). The effect of lintnerization on cereal starch granules. *Food Research*
426 *International*, 35, 665-680.

- 427 Jiang, M., Hong, Y., Gu, Z., Cheng, L., Li, Z., & Li, C. (2018). Effects of acid hydrolysis intensity on the
428 properties of starch/xanthan mixtures. *International Journal of Biological Macromolecules*, 106,
429 320-329.
- 430 Jones, L. R., & Riddick, J. A. (1957). Colorimetric determination of 1,2-propanediol and related compounds.
431 *Analytical Chemistry*, 29, 1214-1216.
- 432 Kaur, B., Ariffin, F., Bhat, R., & Karim, A. A. (2012). Progress in starch modification in the last decade. *Food*
433 *Hydrocolloids*, 26, 398-404.
- 434 Kaur, L., Singh, N., & Singh, J. (2004). Factors influencing the properties of hydroxypropylated potato
435 starches. *Carbohydrate Polymers*, 55, 211-223.
- 436 Kavitha, R., & BeMiller, J. N. (1998). Characterization of hydroxypropylated potato starch. *Carbohydrate*
437 *Polymers*, 37, 115-121.
- 438 Kim, H.-Y., Lee, J. H., Kim, J.-Y., Lim, W.-J., & Lim, S.-T. (2012). Characterization of nanoparticles
439 prepared by acid hydrolysis of various starches. *Starch - Stärke*, 64, 367-373.
- 440 Lawal, O. S. (2009). Starch hydroxyalkylation: Physicochemical properties and enzymatic digestibility of
441 native and hydroxypropylated finger millet (eleusine coracana) starch. *Food Hydrocolloids*, 23,
442 415-425.
- 443 Lawal, O. S. (2011). Hydroxypropylation of pigeon pea (cajanus cajan) starch: Preparation, functional
444 characterizations and enzymatic digestibility. *LWT - Food Science and Technology*, 44, 771-778.
- 445 Lee, H. L., & Yoo, B. (2011). Effect of hydroxypropylation on physical and rheological properties of sweet
446 potato starch. *LWT - Food Science and Technology*, 44, 765-770.
- 447 Li, H., Gidley, M. J., & Dhital, S. (2019). High-amylose starches to bridge the “fiber gap”: Development,
448 structure, and nutritional functionality. *Comprehensive Reviews in Food Science and Food Safety*, 18,

- 449 362-379.
- 450 Li, L., Hong, Y., Gu, Z., Cheng, L., Li, Z., & Li, C. (2018). Effect of a dual modification by
451 hydroxypropylation and acid hydrolysis on the structure and rheological properties of potato starch.
452 *Food Hydrocolloids*, 77, 825-833.
- 453 Li, M., Liu, P., Zou, W., Yu, L., Xie, F., Pu, H., Liu, H., & Chen, L. (2011). Extrusion processing and
454 characterization of edible starch films with different amylose contents. *Journal of Food Engineering*,
455 106, 95-101.
- 456 Li, Y., Liu, P., Ma, C., Zhang, N., Shang, X., Wang, L., & Xie, F. (2020). Structural disorganization and chain
457 aggregation of high-amylose starch in different chloride salt solutions. *ACS Sustainable Chemistry &*
458 *Engineering*.
- 459 Lin, M., Shang, X., Liu, P., Xie, F., Chen, X., Sun, Y., & Wan, J. (2016). Zinc chloride aqueous solution as a
460 solvent for starch. *Carbohydr Polym*, 136, 266-73.
- 461 Liu, H., Ramsden, L., & Corke, H. (1999). Physical properties and enzymatic digestibility of
462 hydroxypropylated ae, wx, and normal maize starch. *Carbohydrate Polymers*, 40, 175-182.
- 463 Liu, H., Yu, L., Xie, F., & Chen, L. (2006). Gelatinization of cornstarch with different amylose/amylopectin
464 content. *Carbohydrate Polymers*, 65, 357-363.
- 465 Liu, P., Li, Y., Shang, X., & Xie, F. (2019). Starch–zinc complex and its reinforcement effect on starch-based
466 materials. *Carbohydrate Polymers*, 206, 528-538.
- 467 Liu, P., Xie, F., Li, M., Liu, X., Yu, L., Halley, P. J., & Chen, L. (2011). Phase transitions of maize starches
468 with different amylose contents in glycerol-water systems. *Carbohydrate Polymers*, 85, 180-187.
- 469 Liu, X., Xiao, X., Liu, P., Yu, L., Li, M., Zhou, S., & Xie, F. (2017). Shear degradation of corn starches with
470 different amylose contents. *Food Hydrocolloids*, 66, 199-205.

- 471 Lopez-Rubio, A., Flanagan, B. M., Gilbert, E. P., & Gidley, M. J. (2008). A novel approach for calculating
472 starch crystallinity and its correlation with double helix content: A combined xrd and nmr study.
473 *Biopolymers*, 89, 761-768.
- 474 Miyazaki, M., Van Hung, P., Maeda, T., & Morita, N. (2006). Recent advances in application of modified
475 starches for breadmaking. *Trends in Food Science & Technology*, 17, 591-599.
- 476 Nakazawa, Y., & Wang, Y.-J. (2003). Acid hydrolysis of native and annealed starches and branch-structure of
477 their naegeli dextrans. *Carbohydrate Research*, 338, 2871-2882.
- 478 Pérez, S., Baldwin, P. M., & Gallant, D. J. (2009). Structural features of starch granules i. In B. James, & W.
479 Roy, *Starch (third edition)* (pp. 149-192). San Diego: Academic Press.
- 480 Qiao, D., Yu, L., Liu, H., Zou, W., Xie, F., Simon, G., Petinakis, E., Shen, Z., & Chen, L. (2016). Insights into
481 the hierarchical structure and digestion rate of alkali-modulated starches with different amylose
482 contents. *Carbohydrate Polymers*, 144, 271-281.
- 483 Seow, C. C., & Thevamar, K. (1993). Internal plasticization of granular rice starch by hydroxypropylation:
484 Effects on phase transitions associated with gelatinization. *Starch - Stärke*, 45, 85-88.
- 485 Sujka, M., & Jamroz, J. (2009). A-amylolysis of native potato and corn starches – sem, afm, nitrogen and
486 iodine sorption investigations. *LWT - Food Science and Technology*, 42, 1219-1224.
- 487 Tajuddin, S., Xie, F., Nicholson, T. M., Liu, P., & Halley, P. J. (2011). Rheological properties of
488 thermoplastic starch studied by multipass rheometer. *Carbohydrate Polymers*, 83, 914-919.
- 489 Tan, I., Flanagan, B. M., Halley, P. J., Whittaker, A. K., & Gidley, M. J. (2007). A method for estimating the
490 nature and relative proportions of amorphous, single, and double-helical components in starch
491 granules by ¹³c cp/mas nmr. *Biomacromolecules*, 8, 885-891.
- 492 Toshio, T. (1968). (American Maize-Products Co) *Hydroxypropyl starch ether*, US3378546A.

- 493 Trinh, K. S., & Dang, T. B. (2019). Structural, physicochemical, and functional properties of electrolyzed
494 cassava starch. *International journal of food science*, 2019.
- 495 Vilaplana, F., Hasjim, J., & Gilbert, R. G. (2012). Amylose content in starches: Toward optimal definition and
496 validating experimental methods. *Carbohydrate Polymers*, 88, 103-111.
- 497 Wang, J., Yu, L., Xie, F., Chen, L., Li, X., & Liu, H. (2010). Rheological properties and phase transition of
498 cornstarches with different amylose/amylopectin ratios under shear stress. *Starch/Stärke*, 62, 667-675.
- 499 Wang, L., & Wang, Y.-J. (2001). Structures and physicochemical properties of acid-thinned corn, potato and
500 rice starches. *Starch - Stärke*, 53, 570-576.
- 501 Wang, S., & Copeland, L. (2015). Effect of acid hydrolysis on starch structure and functionality: A review.
502 *Crit Rev Food Sci Nutr*, 55, 1081-97.
- 503 Wang, Y.-J., Truong, V.-D., & Wang, L. (2003). Structures and rheological properties of corn starch as
504 affected by acid hydrolysis. *Carbohydrate Polymers*, 52, 327-333.
- 505 Woggum, T., Sirivongpaisal, P., & Wittaya, T. (2015a). Characteristics and properties of hydroxypropylated
506 rice starch based biodegradable films. *Food Hydrocolloids*, 50, 54-64.
- 507 Woggum, T., Sirivongpaisal, P., & Wittaya, T. (2015b). Characteristics and properties of hydroxypropylated
508 rice starch based biodegradable films. *Food Hydrocolloids*, 50, 54-64.
- 509 Xie, F., Flanagan, B. M., Li, M., Truss, R. W., Halley, P. J., Gidley, M. J., McNally, T., Shamshina, J. L., &
510 Rogers, R. D. (2015). Characteristics of starch-based films with different amylose contents plasticised
511 by 1-ethyl-3-methylimidazolium acetate. *Carbohydrate Polymers*, 122, 160-168.
- 512 Xie, F., Yu, L., Su, B., Liu, P., Wang, J., Liu, H., & Chen, L. (2009). Rheological properties of starches with
513 different amylose/amylopectin ratios. *Journal of Cereal Science*, 49, 371-377.
- 514 Yang, J., Xie, F., Wen, W., Chen, L., Shang, X., & Liu, P. (2016). Understanding the structural features of

- 515 high-amylose maize starch through hydrothermal treatment. *International Journal of Biological*
516 *Macromolecules*, 84, 268-274.
- 517 Yu, L., & Christie, G. (2005). Microstructure and mechanical properties of orientated thermoplastic starches.
518 *Journal of Materials Science*, 40, 111-116.
- 519 Zhang, B., Zhao, Y., Li, X., Li, L., Xie, F., & Chen, L. (2014). Supramolecular structural changes of waxy and
520 high-amylose cornstarches heated in abundant water. *Food Hydrocolloids*, 35, 700-709.
- 521 Zhang, H., Zhou, X., He, J., Wang, T., Luo, X., Wang, L., Wang, R., & Chen, Z. (2017). Impact of
522 amylosucrase modification on the structural and physicochemical properties of native and
523 acid-thinned waxy corn starch. *Food Chemistry*, 220, 413-419.
- 524 Zhang, L., Wang, Y., Liu, H., Yu, L., Liu, X., Chen, L., & Zhang, N. (2013). Developing hydroxypropyl
525 methylcellulose/hydroxypropyl starch blends for use as capsule materials. *Carbohydrate Polymers*, 98,
526 73-79.
- 527 Zou, W., Yu, L., Liu, X., Chen, L., Zhang, X., Qiao, D., & Zhang, R. (2012). Effects of amylose/amylopectin
528 ratio on starch-based superabsorbent polymers. *Carbohydrate Polymers*, 87, 1583-1588.
- 529

Highlights:

- ✓ Regular and high-amylose maize starches (RMS and HAMS) were dually modified
- ✓ HAMS had higher hydroxypropyl molar substitution (MS) than RMS
- ✓ Acid hydrolysis weakly affected MS and but strongly impacted rheological properties
- ✓ Hydroxypropylation largely decreased the solution viscosity for HAMS
- ✓ The effect of hydroxypropylation on the solution viscosity of RMS was insignificant

The authors declare that there is no conflict of interest regarding the publication of this article.

Journal Pre-proof